

Gravitational lensing as a probe of compact object population in the Galaxy

S. Osłowski¹ R. Moderski² T. Bulik^{1,2} and K. Belczynski^{3,4}

¹ Astronomical Observatory, Warsaw University, Aleje Ujazdowskie 4, 00478 Warsaw, Poland

² Nicolaus Copernicus Astronomical Center, Bartycka 18, 00716 Warsaw, Poland

³ Department of Astronomy, New Mexico State University, Frenger Mall, Las Cruces, NM USA

⁴ Tombaugh Fellow

Received date / Accepted date

ABSTRACT

Aims. The population of solitary compact objects in the Galaxy is very difficult to investigate. In this paper we analyze the possibility of using microlensing searches to detect and to analyze the properties of the solitary black holes and neutron stars.

Methods. Evolution of single and binary stars is considered using the StarTrack population synthesis code. We investigate the properties of the Galactic population of compact objects numerically.

Results. We find that the compact object lensing events are concentrated in a region with the radius of ≈ 5 degrees around the Galactic center. The distribution of masses of the lenses for the models we consider differs but only slightly from the underlying mass distribution. The expected detection rates are of the order of a few per year.

Key words. Gravitational lensing, Galaxy: stellar content

1. Introduction

The stellar evolution models predict the Galactic population of compact objects - neutron stars and black holes - numbers somewhere between 10^7 and 10^9 objects. Most of them are solitary and only a small fraction resides in binaries. A small fraction of solitary neutron stars is visible as radio pulsars. Some black holes in binaries are actively accreting and are observable mainly as X-ray transients, however most of the black hole population has not been yet seen. The properties of black holes population in our galaxy depend on the history of star formation rate, evolution of metallicity and on the initial mass function and on details of compact object formation in supernovae explosions.

The properties of the population of solitary black holes can only be investigated indirectly, through observations of their interaction with the interstellar matter or light emitted by stars. Solitary black holes should be accreting gas from the ISM. Therefore some of them should be observable in X-rays (Agol & Kamionkowski 2002; Beskin & Karpov 2005). The luminosity in X-rays shall on one hand be smaller than for solitary neutron stars where the surface emission plays a significant role, but on the other hand it may be increased due to smaller velocities and higher mass of black holes in comparison with neutron stars. The searches for such objects have not been successful yet.

Solitary black holes are also detectable with current microlensing searches (Paczynski 2003) like OGLE (Udalski 2003) and MOA (Bond et al. 2001). These campaigns have already yielded several candidate black holes detections. Bennett et al. (2002) has presented two events: MACHO-96-BLG-5 and MACHO-98-BLG-6, with the mass estimates $6_{-3}^{+10} M_{\odot}$ and $6_{-3}^{+7} M_{\odot}$ respectively. Mao et al. (2002) showed that OGLE-1999-BUL-32 identified also as MACHO-96-BLG-22 is a black

hole candidate with the minimum mass of $10.5 M_{\odot}$. A further search for X-rays from MACHO-96-BLG-5 (Maeda et al. 2005) yielded an upper limit corresponding to the luminosity of less than $(8 - 9) \times 10^{-10} L_{Edd}$. A recent likelihood analysis of 22 microlensing events Poindexter et al. (2005) lead to confirmation of the black hole candidate MACHO-99-BLG-22, while the other candidates are less probable.

The sample of the microlensing compact objects and black hole candidates will increase with time. It is therefore interesting to see what constraints can be imposed on the models of black hole formation and evolution by these observations. In this paper we present a simulation of the stellar evolution leading to production of solitary black holes in our galaxy. We analyze two scenarios: the single stellar evolution and the formation of solitary black holes through disruption of binaries. We then analyze the motion of black holes in the galactic potential and search for possible microlensing observable from the Earth.

In section 2 we present the basic ingredients of the calculation: the stellar evolution model, the galactic potential and mass distribution used, and the lensing search algorithm. Section 3 contains the results and section 4 the discussion.

2. Description of the model

2.1. Compact object formation

The single star evolution is modeled using the formulae of Hurley et al. (2000) and we use the StarTrack population synthesis code (Belczynski et al. 2002a) for modelling binary evolution. The StarTrack population synthesis code was initially developed for the study of double compact object mergers in the context of GRB progenitors (Belczynski et al. 2002a) and gravitational-wave inspiral sources (Belczynski et al. 2002b). In recent years StarTrack has undergone major updates and re-

Table 1. Models of black hole formation considered in this paper

Model	Description
A	Standard
W05	stellar winds decreased by 0.5
K0	Black holes receive no kicks
K1	Black holes receive full kicks
C	Hertzsprung gap stars can be donors in CE phase
S	Only single stars
M	Black holes from mergers

visions in the physical treatment of various binary evolution phases. The new version has already been tested against observations and detailed evolutionary calculations (Belczynski et al. 2006), and has been used in various applications. The most important updates for compact object formation and evolution include: a full numerical approach to binary evolution due to tidal interactions and coupling calibrated using high mass X-ray binaries and open cluster observations, a detailed treatment of mass transfer episodes fully calibrated against detailed calculations with a stellar evolution code, updated stellar winds for massive stars, and the latest determination of natal kick velocity distribution for neutron stars (Hobbs et al. 2005). For disrupted (by supernova explosion) binaries we follow trajectories of components as described in Belczynski et al. (2006). In the helium star evolution, which is of a crucial importance for the formation of new classes of double compact objects, e.g., Ivanova et al. (2003), we have applied a conservative treatment matching closely the results of detailed evolutionary calculations. The NS-NS progenitors are followed and checked for any potential Roche lobe overflow (RLOF). While in the mass transfer phase, systems are examined for potential development of dynamical instability, in which case the systems are evolved through a common envelope phase. We treat common envelope events through the energy formalism (Webbink 1984; Belczynski et al. 2002b), where the binding energy of the envelope is determined from the set of He star models calculated with the detailed evolutionary code by Ivanova et al. (2003). For some systems we observe, as before, extra orbital decay leading to the formation of very tight short lived double compact object binaries. However, since the progenitor evolution and the final RLOF episodes are now followed in much greater detail, we note significant differences from our earlier studies. For a detailed description of the revised code we refer the reader to Belczynski et al. (2006).

The simplest scenario leading to a single compact object is through evolution of single stars. In this case we put the newly formed star in the galactic disc with its velocity drawn from an appropriate distribution after the supernova event.

An important additional scenario follows a disruption of a binary as a result of a first supernova explosion. A large fraction of binaries containing massive stars is disrupted in this way. This leads to a formation of a single compact object and a single companion which may still be massive enough to produce another compact object. We assume that the first supernova explosion takes place in the galactic disk. We follow the motion of the single star until it produces another compact object.

A much smaller contribution comes from the disruption of a binary during the second supernova explosion. In this case two single compact objects are formed. We follow the motion of the system after the first supernova until the second one. Thus the newly formed single compact objects start at the actual location of the second supernova with appropriate velocities.

Finally, we also investigate black hole formation through mergers. This includes mergers of stars during their nuclear evolution, as well as mergers of a compact object with a massive companion as a result of binary interaction. In the first case we assume that a single star is formed with the mass equal to the sum of the masses of the two merging components and we evolve this star neglecting the potential changes in metallicity. In the latter case we assume that a single black hole is formed with the mass equal to the sum of the masses of the compact object and the core of the companion while the envelope is expelled. The newly formed black holes do not gain additional velocities during mergers.

We ignore the contribution of double black hole systems, and single black holes formed in mergers of double black holes as they represent a much smaller population than the ones mentioned above.

We consider several models of binary evolution to assess the sensitivity of the results. We decrease the strength of the stellar winds which affects mainly the masses of the newly formed compact objects (model W05). A second parameter that may influence the results significantly is the distribution of the kicks received by the newly formed compact object. Apart from the standard model in which the value of the kick is decreased with increasing fall-back mass, we consider two extreme cases: in first black holes receive no kicks at all (model K0), and in the second one kick distribution regardless of their mass is the same as for neutron stars (model K1). Finally in model C we allow for the common envelope evolution initiated by stars passing through the Hertzsprung gap.

The list of the models considered is shown in Table 1.

2.2. Galactic model

We consider a model of the Galaxy consisting of three components: bulge, disk, and halo. The bulge and disk potential are described by the Miyamoto & Nagai (1975) type potential (Paczynski 1990; Bulik et al. 1999)

$$\Phi(r, z) = \frac{GM}{\sqrt{R^2 + (a + \sqrt{z^2 + b^2})^2}}, \quad (1)$$

where M is the mass of a given component, $R = \sqrt{x^2 + y^2}$, and a, b are the parameters. The halo is described by the density distribution $\rho = \rho_c [1 + (r/r_c)^2]^{-1}$ with a cutoff at $r_{cut} = 100$ kpc above which the halo density is zero. The corresponding potential for $r < r_{cut}$ is

$$\Phi(r) = -\frac{GM_h}{r_c} \left[\frac{1}{2} \ln \left(1 + \frac{r^2}{r_c^2} \right) + \frac{r_c}{r} \arctan \left(\frac{r}{r_c} \right) \right] \quad (2)$$

We use the following values of the parameters (Blaes & Rajagopal 1991) describing the potential: $a_1 = 0$ kpc, $b_1 = 0.277$ kpc, $a_2 = 4.2$ kpc, $b_2 = 0.198$ kpc, $M_1 = 1.12 \times 10^{10} M_\odot$, $M_2 = 8.78 \times 10^{10} M_\odot$, $M_h = 5.0 \times 10^{10} M_\odot$, and $r_c = 6.0$ kpc.

The distribution of stars in the disk is assumed to be that of a young disc (Paczynski 1990). The radial and vertical distributions are independent i.e. the distributions factor out:

$$P(R, z) \propto R(R) dR p(z) dz, \quad (3)$$

where the radial distribution is $p(R) \propto \exp(-R/R_{exp})$, and $R_{exp} = 4.5$ kpc, and we introduce an upper cutoff at $R_{max} = 20$ kpc. The vertical distribution is exponential $p(z) \propto \exp(-z/75$ pc)

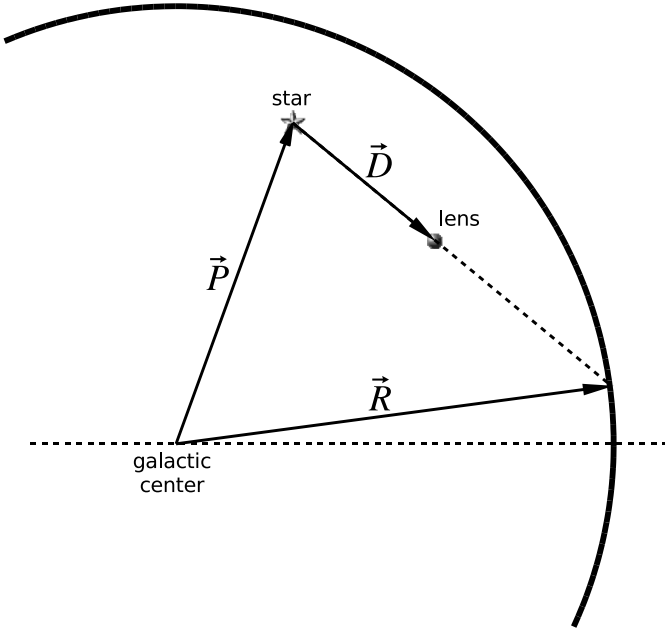


Fig. 1. Geometry of the lensing event. Star and the lens are located inside a sphere of radius R equal to the radius of the Earth's orbit. Vector \vec{P} denotes the position of the star in the galaxy, while \vec{D} is a star-lens vector. We look for a situation when star-lens line crosses the Earth's orbit during the evolution of the system.

. This is not a self consistent approach since the matter density corresponding to the disk potential is not the same as the stellar density. A self consistent approach has been investigated by Bulik et al. (1998) using the potentials calculated by Kuijken & Gilmore (1989).

2.3. Lens search algorithm

A naive search for lenses i.e. testing for events when a star and a compact object are aligned with Earth on its galactic orbit would require nearly infinite computational resources. Therefore we use the following lens search algorithm. We look for the lens events that take place anywhere on the galactic orbit of the Earth. This is much easier computationally as this approach make use of the cylindrical symmetry of the Milky Way.

We assume that the Earth's orbit is circular with the radius of 8.5 kpc. Let us consider a sphere of radius $R = 8.5$ kpc (which is equal to Earth's galactic orbit radius) and centered in the center of the galaxy. Let us also consider a star-lens system located somewhere in the galaxy. The position of the system is characterized by two vectors: \vec{P} - the position vector of the star in the galaxy, and \vec{D} - the star-lens vector (see Fig. 1). We search for a point Q in which the line passing through the position of the star and the lens pierces the sphere. In principle we look for a factor t which satisfies the condition

$$|\vec{P} + t\vec{D}| = R. \quad (4)$$

Eq. (4) is a quadratic equation in t

$$(\vec{P} + t\vec{D}) \cdot (\vec{P} + t\vec{D}) = R^2, \quad (5)$$

$$D^2 t^2 + 2\vec{D} \cdot \vec{P} t + (P^2 - R^2) = 0. \quad (6)$$

Providing that $\Delta = 4(\vec{D} \cdot \vec{P})^2 - 4D^2(P^2 - R^2) \geq 0$ the Eq. (6) has a formal solution:

$$t_{1,2} = \frac{1}{D^2} \left[-\vec{D} \cdot \vec{P} \pm \sqrt{(\vec{D} \cdot \vec{P})^2 - D^2(P^2 - R^2)} \right]. \quad (7)$$

Now, for each pair of a star and a compact object, we calculate Δ taking into account their positions at the beginning and at the end of a calculation step. If $\Delta > 0$ we calculate Δ' from the position of the pair at the end of the step, which in our calculations was one month. If it is also positive, then we calculate both $t_{1,2}$ and $t'_{1,2}$, respectively. We are only interested in a configuration for which $t_{1,2} > 1$ and $t'_{1,2} > 1$. If $t < 0$ the compact object is located behind the star, and for $0 \leq t \leq 1$ the compact object and the star reside on the opposite sides of the sphere. In both such cases the lensing event cannot be observed on Earth. For both t and t' we then calculate positions of the points where star-lens line crosses the sphere at the beginning and at the end of the examined evolution period. The lensing event happens if these points are located in different hemispheres ($z'z < 0$).

This algorithm is not sensitive to some special configurations when during the evolution star or compact object are located outside the sphere at very high azimuthal angles (as seen from Earth). We checked for these special occasions with two additional algorithms. We conclude that such events are extremely rare (there was not even one such case) and does not influence our results.

2.4. Lensing rate

In order to estimate the true lensing rate one has to scale the number of the lensing events found in the simulation to match the physical conditions in our Galaxy. There are two scaling factors involved. One results from the number of simulated stars and compact objects and the second from the fact that we look for the lensing events that happen on the whole Earth's orbit. Let us denote the Earth orbital period in the Milky way as $P = 250$ Myrs. Let the true number of star in the Milky Way be $N_{11}^* \times 10^{11}$, and $f_{lens} = 10^{-2} f_{lens,-2}$ represent the fraction of the stars in the galaxy that can be detected by lens search experiments. and the number of compact objects in the Galaxy $N_8^{CO} \times 10^8$. Our simulations include 10^6 stars that can be lensed in the Galactic potential.

Thus the expected rate of lenses due to the compact objects is

$$R = 4 \times 10^2 f_{lens,-2} N_{11}^* N_8^{CO} \frac{N_{lens}}{N_{sim}}, \quad (8)$$

where N_{sim} is the number of compact objects (potential lenses) in the simulation, and N_{lens} is the number of lenses we find in one year.

3. Results

Using Startrack population synthesis code we evolved 10^5 binary systems, obtaining data about compact objects (neutron stars and black holes). We put those objects (only solitary, from disrupted systems) into the model Galaxy. We also randomly introduced 10^6 stars in the Milky Way. All the stars were then evolved for 10Gy in Galactic potential taking into account the initial velocities that the compact objects received at birth due to asymmetric kicks and disruptions of the binary systems Blaauw (1961). We then searched for lensing events that take place anywhere on the Earth orbit in the galaxy in one year of simulation.

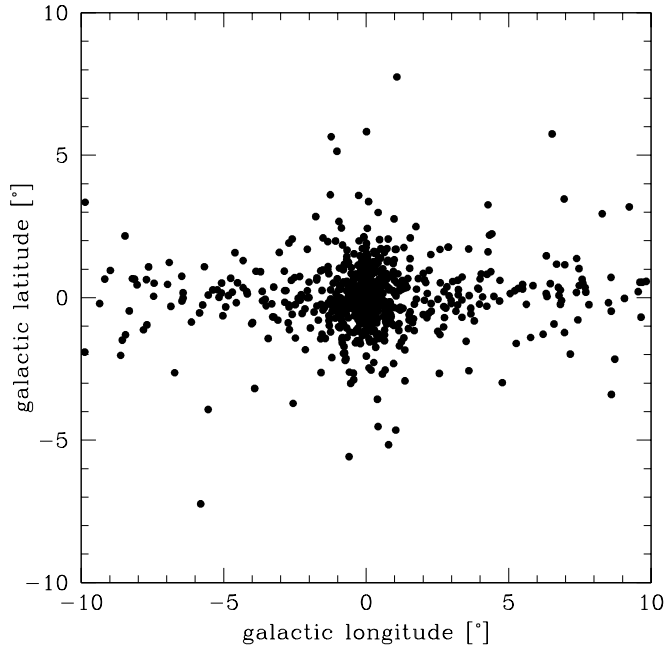


Fig. 2. Skymap of the simulated lensing events for the standard model of compact object formation. The skymaps in the two alternative models look similar.

Table 2. The results of the lens search simulations and the expected galactic lensing rates.

Model	N_{sim}	N_{lens}	Rate[yr ⁻¹]
A	76399	826	4.3
W0.5	73575	757	4.1
K0	26619	584	8.7
K1	73907	687	3.7
C	81327	887	4.3
S	60340	1368	9.0
M	8170	194	9.5

The resulting rates, calculated using equation 8, are presented in Table 1 for each model assuming that $N_{11}^* = 1$, and $N_8^{CO} = 1$. The typical values obtained are a few tens per year, however these expected rates have to be considered as rough estimates given the number of assumptions used in equation 8. Note that the Table gives the values of the rates assuming that all compact objects are formed in the particular scenario.

In each simulation we have noted the positions of the lensing events on the sky. We present the skymaps of these position in Figure 2. The lenses are strongly concentrated around the galactic center. In Figure 3 we present the cumulative distribution of the fraction of events as a function of the distance from the Galactic Center. Typically 70% of the lensing events take place within $\approx 5^\circ$ from the Galactic Center, while a fraction 0.9 of the events happens within 20° .

We also note the mass of the gravitational lens for each lensing event. In Figures 4 and 5 we present the intrinsic distributions of masses of compact objects for each model and the mass distribution of lenses. In the case of models S, M, K0, and K1 the distributions are either quite similar. They do differ in the case of remaining models. But if they differ then they do in the same manner: the distribution of observed masses shows a deficiency

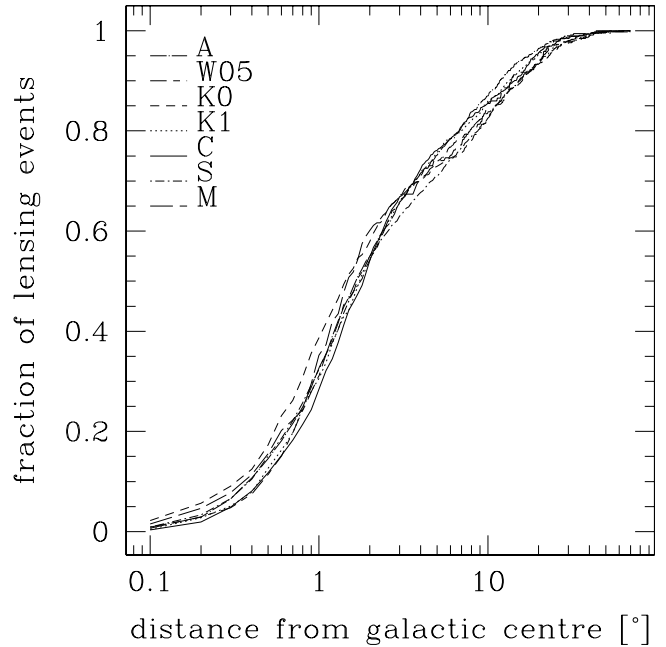


Fig. 3. Cumulative distributions of the angular distance lensing events from the Galactic Center for the models considered in the paper.

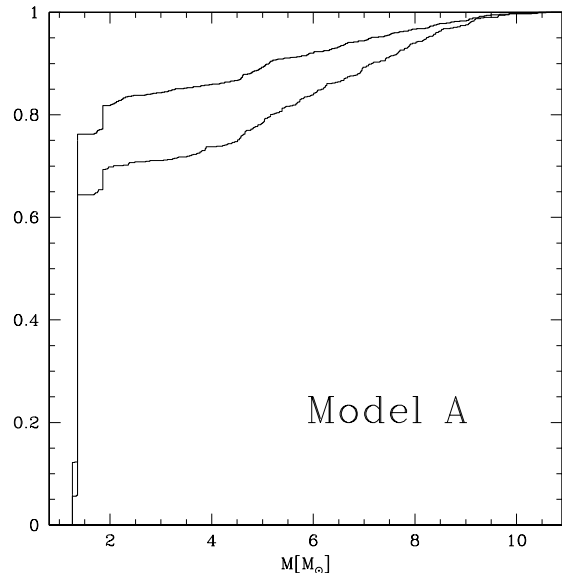


Fig. 4. The cumulative distributions of masses of compact objects in the standard model A. The thick line denotes the intrinsic distribution of compact object masses while the thin line corresponds to the distribution of measured masses of the lenses. Each plot is labeled by the model as in Table 1.

of low mass compact objects (neutron stars) and an increased fraction of high mass objects (black holes). The distributions are similar for the models in which the velocities of compact objects weakly depend on their masses: K0, and K1.

In the cases when the distributions differ the suppression of low mass compact objects is not more than about 20% in relation to the high mass compact objects.

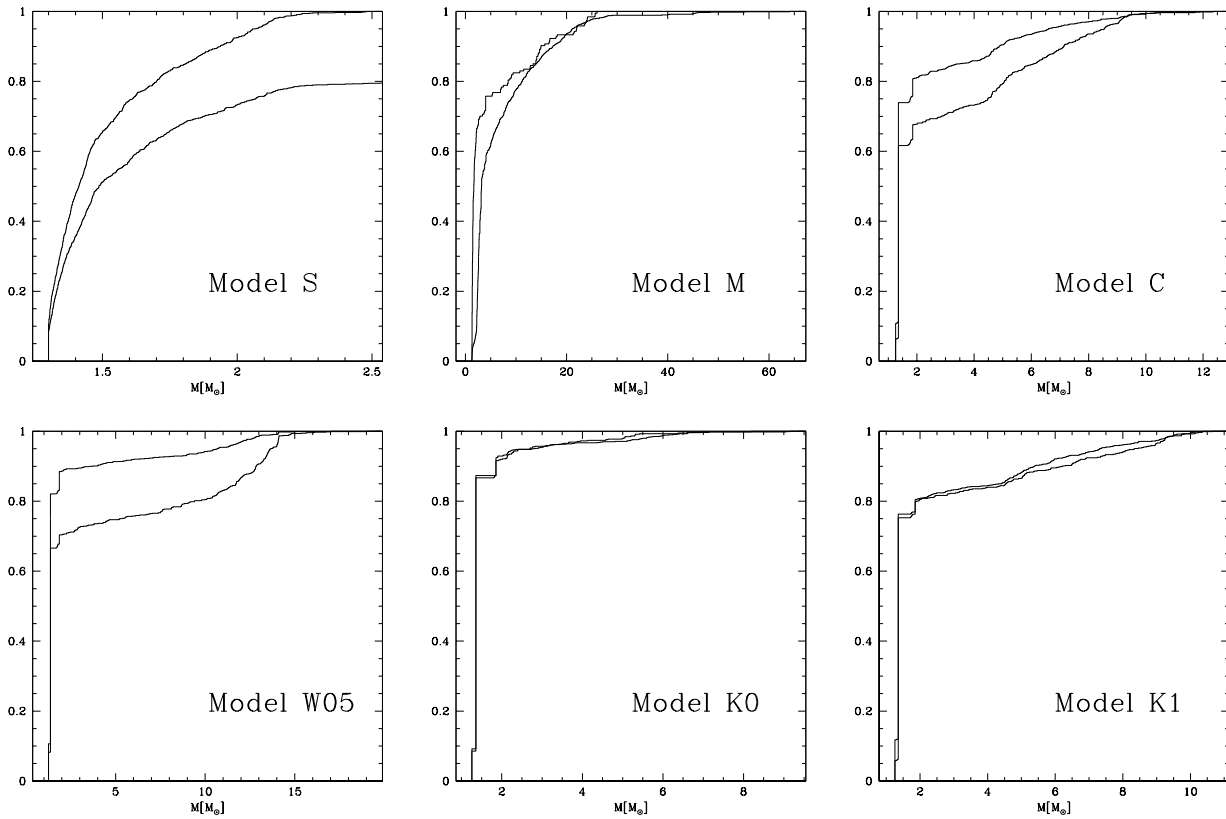


Fig. 5. Same as Figure 4 but for the remaining models.

4. Summary

We have considered several scenarios leading to formation of galactic compact objects and calculated their initial velocity distributions. We then simulate the spatial and velocity distributions of them in our Galaxy. Each model yields a different compact objects mass distribution and may have a different distribution of velocities. We simulate the microlensing events and note both mass and position for each one.

We estimate the rates of lensing events due to compact objects. These estimates show that they can be observed. The rates in Table 2 must be taken as very rough estimates. There are some poorly known factors that are included in these rates - see equation 8. One should note that the fraction of objects detectable by the lens searches f_{lens} can be increased for the searches conducted in the infrared. However, we know that there already are some events which can be interpreted as microlensing events by black holes.

In the simulations the robust result is the distribution of lensing events in sky. All the events are well concentrated around the Galactic center. Thus the lens searches should concentrate on this region. This is probably due to the fact that the dominant factor determining the position on the sky is the density of the lensed stars and not lenses themselves.

Finally, we find that the observed mass distributions differ by less than 20% from the intrinsic one. The observations of several gravitational lenses from black holes or neutron stars should lead to relatively good estimate of the intrinsic compact object mass distribution. The observation of the mass distribution of compact objects is extremely important since this is a unique way to probe the final stages of the massive stars evolution. Observations of

black holes in massive accreting binaries may suffer from numerous selection effects and probably do not reflect the underlying intrinsic distribution.

The lensing events due to massive lenses will have long duration and therefore require long observational campaigns. We emphasize the importance of such searches, as their potential results will have a very significant relevance for the theory of compact object formation and models of massive star evolution.

Acknowledgements. This research was supported by the KBN grant 1P03D02228. The authors thank A. Udalski for useful comments on the manuscript. We are also grateful to A. Sadowski for help with the merger calculation.

References

- Agol, E. & Kamionkowski, M. 2002, MNRAS, 334, 553
- Belczynski, K., Bulik, T., & Rudak, B. 2002a, ApJ, 571, 394
- Belczynski, K., Kalogera, V., & Bulik, T. 2002b, ApJ, 572, 407
- Belczynski, K., Kalogera, V., Rasio, F., et al. 2006, submitted, astro-ph/0511811
- Belczynski, K., Sadowski, A., Rasio, F. A., & Bulik, T. 2006, ApJ, 650, 303
- Bennett, D. P., Becker, A. C., Quinn, J. L., et al. 2002, ApJ, 579, 639
- Beskin, G. M. & Karpov, S. V. 2005, A&A, 440, 223
- Blaauw, A. 1961, Bull. Astron. Inst. Netherlands, 15, 265
- Blaes, O. & Rajagopal, M. 1991, ApJ, 381, 210
- Bond, I. A., Abe, F., Dodd, R. J., et al. 2001, MNRAS, 327, 868
- Bulik, T., Belczyński, K., & Zbijewski, W. 1999, MNRAS, 309, 629
- Bulik, T., Lamb, D. Q., & Coppi, P. S. 1998, ApJ, 505, 666
- Hobbs, G., Lorimer, D. R., Lyne, A. G., & Kramer, M. 2005, MNRAS, 360, 974
- Hurley, J. R., Pols, O. R., & Tout, C. A. 2000, MNRAS, 315, 543
- Ivanova, N., Belczynski, K., Kalogera, V., Rasio, F. A., & Taam, R. E. 2003, ApJ, 592, 475
- Kuijken, K. & Gilmore, G. 1989, MNRAS, 239, 571
- Maeda, Y., Kubota, A., Kobayashi, Y., et al. 2005, ApJ, 631, L65
- Mao, S., Smith, M. C., Woźniak, P., et al. 2002, MNRAS, 329, 349

- Miyamoto, M. & Nagai, R. 1975, PASJ, 27, 533
Paczynski, B. 1990, ApJ, 348, 485
Paczynski, B. 2003, astro-ph/00306564
Poindexter, S., Afonso, C., Bennett, D. P., et al. 2005, ApJ, 633, 914
Udalski, A. 2003, Acta Astronomica, 53, 291
Webbink, R. F. 1984, ApJ, 277, 355